Original Article

Determining Area Affected by Corona in Lung Computed Tomography Images by Three-phase Level Set and Shearlet Transform

Abstract

Background: The COVID-19 pandemic has created a critical global situation, causing widespread challenges and numerous fatalities due to severe respiratory complications. Since lung involvement is a key factor in COVID-19 diagnosis and treatment, accurate identification of infected regions in lung images is essential. **Methods:** We propose a multiphase segmentation method based on the level set framework to determine lunginvolved areas. The shearlet transform, a high-precision directional multiresolution transform, is employed to guide the gradient flow in the level set formulation. Additionally, the phase stretch transform (PST) is applied to enhance the contrast between infected and healthy regions, improving convergence speed during segmentation. **Results:** The proposed algorithm was tested on 500 lung images. The method accurately identified infected areas, enabling precise calculation of the percentage of lung involvement. The use of the shearlet transform also allowed clear delineation of ground-glass opacity boundaries. **Conclusion:** The proposed multiphase level set method, enhanced with shearlet and phase stretch transforms, effectively segments COVID-19–infected lung regions. This approach improves segmentation accuracy and computational efficiency, offering a reliable tool for quantitative lung involvement assessment.

Keywords: *Contrast stretch, coronavirus, segmentation, shearlet transform, similarity measurement, three-phase level set*

Submitted: 06-Feb-2025 **Revised:** 25-Jun-2025 **Accepted:** 14-Jul-2025 **Published:** 01-Dec-2025

Nasser Aghazadeh[1,2,3], Parisa Noras[1], Sevda Moghaddasighamchi[1,4]

[1]Department of Mathematics, Azarbaijan Shahid Madani University, Tabriz, Iran, [2]Department of Mathematics, Izmir Institute of Technology, Izmir, Türkiye, [3]Center for Theoretical Physics, Khazar University,41 Mehseti Street, Baku, AZ1096, Azerbaijan, [4]Institute for Numerical and Applied Mathematics, Georg-August-University of Göttingen, Göttingen, Germany

Address for correspondence:
Prof. Nasser Aghazadeh, Department of Mathematics, Azarbaijan Shahid Madani University, Tabriz, Iran. E-mail: nasseraghazadeh@iyte.edu.tr

Introduction

Since the infection of COVID-19 has seriously posed a problem to human health and its effects on the lungs can make human life impossible, understanding the involvement of lung tissue in COVID-19 is essential for diagnosis, treatment, and management of the disease. A quick method for visualizing lung abnormalities is using chest images, including X-rays and computed tomography (CT) scans, which play a vital role. Chest X-rays (CXRs) may show areas of consolidation or opacity. CT sequences are more specific, often revealing ground glass opacities (GGOs), reticular patterns, and consolidations typical of COVID-19 pneumonia. However, experts can interpret the results in a time-consuming manner. Therefore, automatic segmentation of COVID-19 X-ray images by computer programs is a crucial tool to aid physicians in diagnosing COVID-19-involved areas promptly and accurately. There are several methods and experiments to diagnose this disease. The common tests performed in Iran to check for this disease are polymerase chain reaction, antibody, and CT scans. Since the number of patients infected with COVID-19 is increasing all over the world, in the absence of the production of appropriate therapeutic drugs or vaccines, it is necessary to identify patients with COVID-19 in its early stages so that patients can be separated from the healthy population and treated as soon as possible. Some studies show that CT scan seems to be a promising and efficient method for diagnosing COVID-19.[1] Moreover, CT images of the lung can show the involved area as gray clouds, whereas healthy parts of the lung are seen in black. Therefore, using methods to distinguish the lung image into healthy and involved parts can be useful for automated diagnosis.

In recent years, many studies have been done on the coronavirus. Aslan[2] used CXR images to detect COVID-19 by a deep learning-based system. He utilized

How to cite this article: Aghazadeh N, Noras P, Moghaddasighamchi S. Determining area affected by corona in lung computed tomography images by three-phase level set and shearlet transform. J Med Sign Sens 2025;15:32.

Access this article online

Website: www.jmssjournal.net

DOI: 10.4103/jmss.jmss_18_25

Quick Response Code:

masks that segment the lung parts in the COVID-19 radiography dataset. Then, the author trained DeepLabV3. By using preprocessing, lung regions have been segmented better. The modified AlexNet has been used for feature extraction. Moreover, the support vector machine was used for classification. As a result, data can be classified into three classes: Normal, Viral Pneumonia, and COVID-19. This method only determines whether one person's chest has been affected by coronavirus. Furthermore, it cannot be done quickly because of using DeepLab.

In Chakraborty and Mali,[3] the authors proposed an approach called SUFEMO, which depends on optimization, type 2 fuzzy logic, and superpixels. Their approach reduces the processing burden that is required to deal with a considerable amount of spatial information by the notion of the superpixel. Their work employed the evolutionary multiobjective optimization approach within a type-2 fuzzy framework. Their approach updates cluster centers without relying on the traditional cluster center update equation, making it independent of the initial choice of cluster centers. To further reduce the computational time required for processing extensive spatial data, they proposed a novel superpixel-based scheme based on the watershed formation, which dealt with computing the local minima from the gradient image.

Additionally, the fuzzy objective function is adapted for detecting COVID-19 using superpixels. Their approach was evaluated using 310 chest CT scan images that were collected from several hospitals. Their work has this flaw in that all pixels have no similar neighbors to use watershed, and it cannot be suitable in terms of noise.

In Hao *et al*.,[4] the authors proposed an improved fruit fly optimization algorithm (EEFOA) where two optimization schemes, elite natural evolution and elite random mutation, were added to the original funding opportunity announcement (FOA). These schemes can efficiently speed the convergence rate and local optima. EEFOA has demonstrated performance compared to FOA. Moreover, in EEFOA, multi-threshold image segmentation based on the two-dimensional histogram of the grayscale images has occurred. Then, entropy was used as an objective function to find the maximum value of the objective. The experimental results of their method show that the EEFOA method can achieve better quality segmentation results and more robustness than FOA. However, the involved area can be better presented in CT images than in X-ray images. Their method is used only on X-ray chest images.

Authors in Karar *et al*.[5] have presented an automatic segmentation of lung CT images by proposing squeeze and excitation networks. Their proposed SE blocks are integrated from deep networks. Their method was examined on 20 CT images plus 1800 slices. It demonstrated strong performance, achieving a Dice score of 0.73, a structural similarity index of 0.98, an enhanced alignment measure of 0.98, and a mean absolute error of 0.06. Their work has been done on CT images, but using networks has led to more time spent detecting coronavirus.

In Madhavi and Supraja,[6] the authors classified the CT images into COVID-19 and non-COVID-19 images using the iterated convolution neural network. The testing data size was 20 images. The training data size was 500, and after the 6th iteration, the performance of convolutional neural networks (CNNs) was degraded. Two or three hidden layers can do it and have achieved higher accuracy in COVID-19 classification than other CNN models. The proposed model reached an improved classification accuracy of 89% at its 5th iteration. However, their method cannot detect the area of the lung that is involved.

In Kalaivani and Seetharaman,[7] the authors presented a three-stage ensemble boosted CNN model. In the first stage, a CNN enhanced the model's performance during the initial dataset processing. In the second stage, the CNN was employed for feature extraction from the images in the training dataset using machine learning methods. Finally, in the third stage, the extracted features were combined using a voting mechanism based on machine learning techniques. This work has detected involved chests from healthy chests. Using neural networks may lead to good results, but it needs a large dataset to ensure true results.

In image segmentation, the edges of images play a decisive role because they can determine the borders of image regions. In computer vision, edge detection refers to the process of identifying points where intensity values have sharp transitions.[8] Edge detection methods can facilitate object identification, feature extraction, region segmentation, and many more.[9,10] Consequently, edge detection is often considered the first step in image understanding. Various edge detection methods exist.[11-14] Classic edge detectors, such as Sobel, Roberts, Prewitt, and Robinson, identify edges by convolving an image with a weighted matrix called a local gradient mask. These masks are derived from the first derivatives of the image. However, these methods often struggle to detect all edges accurately. On the other hand, other classic edge detectors like Marr–Hildreth detect edge points by identifying zero-crossings in the Laplacian of Gaussian. Despite this, they frequently produce false edge points and are less effective at accurately localizing curved edges.[15,16]

The Canny edge detector, which utilizes the first derivative of a Gaussian filter, surpasses earlier edge detection methods by pinpointing locations where the image gradient exhibits a local maximum. Its performance depends on σ (the control parameter in the Canny filter for edge detection). The Canny method was optimal for detection, localization, and the number of responses for edge points.[17]

In recent decades, wavelets have been used for edge detection due to their multiscale properties, which provide

an advantage over classic edge detectors.[18,19] They excel at edge detection due to their multiscale nature. This means they can analyze an image at different levels of detail, capturing edges at various scales. In addition, using a multiscale representation eliminates the need to find the appropriate scale for manual scale selection (or σ) required by the Canny method.

However, a limitation of using wavelets for edge detection is that the wavelet transform calculates the image gradient only in horizontal and vertical directions, omitting information from other directions. Consequently, wavelets have limited effectiveness in detecting directional features, such as edges. Several methods have been introduced in recent years to address this issue, including contourlets, complex wavelets, ridgelets, curvelets, and shearlets. Among these methods, the shearlet representation is notable because it utilizes a single or finite set of generating functions and provides efficient algorithmic implementations for discrete data, such as digital images.[20-23] Therefore, in this study, the shearlet system has been used for gradient computation.

Edge detection by one thresholding value has this problem: if the thresholding value is selected as a high value, strong edges will be determined, and if the thresholding value is lower, in addition to strong edges, weak edges may be determined. If the image has some segments and each of them has edges that different threshold values can obtain, maybe not all the edges of one segment are determined. To overcome this problem, in the first algorithm in this paper, the image is segmented into subimages based on the similarity with the neighborhood, and then in each sub-image, an edge detection procedure by shearlets is applied. In addition to strong and weak edges, hidden edges can be determined by this work. In the second scheme, a contrast stretch transform was applied to the low-pass part of the image. Then, the multiphase segmentation in Algorithm 2 and highlighting edges guided by Algorithm 1 can determine the affected regions by the corona. By this work, the difference between pixels has been increased; therefore, we can get better results for edge detection by using shearlets. Moreover, to increase the difference in grayscale values, we have used contrast stretching on the low-pass part of the shearlet coefficients. Furthermore, we have used these algorithms to detect coronavirus-involved areas in lung CT images. The interesting thing is that the corona areas form separate phases in the multiphase method. Moreover, we have applied Algorithm 2 on each lobe separately with different sigma values for better results. We have gathered our data from Ayatollah Taleghani Hospital in Urmia. It contains over 700 images of the lungs of people with pneumonia caused by COVID-19. We have examined our algorithms on 500 chosen images from that database. The study's dataset comprises over 700 lung CT scan slices from patients diagnosed with COVID-19 pneumonia. However, not all images in this collection provided equal relevance for our method's objective. A considerable number of images were from upper lung areas showing no signs of pneumonia, where the lungs appeared entirely healthy, or from lower lung regions where the infection had severely progressed, offering no clear healthy lung tissue. In contrast, the middle lung regions exhibited a combination of healthy and infected tissue, featuring visible COVID-19 lesions, normal lung parenchyma, blood vessels, and other anatomical structures. These middle lung images were most suitable for assessing our proposed method, which aims to differentiate infected regions from healthy lung tissue using a level set approach. Therefore, we selected 500 representative images from this subset that best captured the challenge our algorithm is designed to address. We believe this focused evaluation provides greater significance than utilizing the entire dataset, much of which would not deliver pertinent information for the analysis.

This paper is structured in the following manner. In Section 2, the shearlet system and shearlet transform have been introduced. In section 3, multiphase segmentation and the proposed algorithms for edge guiding and segmentation of corona areas are presented, and experimental results are presented. Eventually, in section 4, the conclusions of our work are discussed.

Shearlet Transform

Multidirectional versions of wavelets are called shearlets, which can extract low- and high-frequency parts of the image in multiresolution form. The shearlet transform is an advanced mathematical technique for analyzing data. Shearlets are essentially a family of functions derived from a few fundamental building blocks. These building blocks are then manipulated through scaling (for adjusting size), shifting (for moving the position), and rotating (for changing the orientation). This process allows shearlets to capture details at different scales and angles in multiresolution analysis. This clever structure leads to efficient algorithms for processing signals and images. They have good results in denoising and edge detection of the images because they can detect singularities in more directions and smooth the images in more directions. Therefore, these properties can lead to better results in segmentation. Hence, first, the definition of shearlets is stated and briefly introduced.

Definition 1: If $\psi \in L^2\left(R^2\right)$ satisfies in the following condition

$$\int_{R^2} \frac{\left|\hat{\psi}\left(\xi_1,\xi_2\right)\right|^2}{\xi_1^2} d\xi_2 d\xi_1 < \infty \quad (1)$$

It is called an admissible shearlet. Note that any function ψ that $\hat{\psi}$ is compactly supported away from the origin is an admissible shearlet. One example of these shearlets is given in the following definition.

Definition 2: Let be $\psi \in L^2\left(R^2\right)$ defined by

$$\hat{\psi}(\xi)=\hat{\psi}(\xi_1,\xi_2)=\hat{\psi}(\xi_1)\hat{\psi}\left(\frac{\xi_2}{\xi_1}\right) \quad (2)$$

Where $\psi_1 \in L^2(R)$ is a discrete wavelet, satisfies the discrete Calderon condition, i.e.

$$\sum_{j\in Z}\left|\hat{\psi}_1\left(2^{-j}\xi\right)\right|^2=1 \quad for \quad a.e. \quad \xi\in R \quad (3)$$

With $\hat{\psi}_1 \in C^{\infty}(R)$ and supp $\hat{\psi}_1 \subseteq \left[\frac{-1}{2},\frac{-1}{16}\right]\cup\left[\frac{1}{16},\frac{1}{2}\right]$, and $\psi_2 \in L^2(R)$ is a bump function such that

$$\sum_{k=-1}^{1}\left|\hat{\psi}_2(\xi+k)\right|^2=1 \quad for \quad a.e. \quad \xi\in[-1,1]. \quad (4)$$

Satisfying $\hat{\psi}_2 \in C^{\infty}(R)$ and supp $\hat{\psi}_2 \subseteq [-1,1]$. Then ψ is called a classical shearlet.

Classic shearlet is a Parseval frame for $L^2(R^2)$. Therefore, the continuous shearlet system $SH(\psi)$, which is defined by

$$SH(\psi)=\left\{\psi_{a,s,t}=T_t D_{A_a} D_{S_s}\psi : a>0, s\in R, t\in R^2\right\} \quad (5)$$

Where D is the dilation operator given by $D_{A_a}\psi(x)=\left|\det A_\alpha\right|^{-1}\psi\left(A_\alpha^{-1}x\right)$, and

$$A_a=\begin{pmatrix}\alpha & 0\\ 0 & \alpha^{1/2}\end{pmatrix}, \quad S_s=\begin{pmatrix}1 & s\\ 0 & 1\end{pmatrix}, \quad T_t\psi(x)=\psi(x-t), \quad t\in R^2 \quad (6)$$

Satisfies a reproducing formula for $L^2(R^2)$.

Definition 3. For $\psi \in L^2(R^2)$, the continuous shearlet transform of $f\in L^2(R^2)$ is the mapping

$$f\in L^2(R^2)\to SH_\psi f(a,s,t)=\langle f,\psi(a,s,t)\rangle, \quad (7)$$

associated with the scale variable $a>0$, the orientation variable $s\in R$, and the location variable $t\in R^2$. One of these shearlet transform coefficients is a low-pass, and the others are high-pass coefficients. In Yi *et al.*,[21] the author has been given the edge detection scheme based on shearlets, which we have used in this paper for comparison.

Multiphase Segmentation

The Level Set Method is a numerical technique for tracking and analyzing moving interfaces and shapes. Introduced by Stanley Osher and Sethian in 1988,[24] this method is widely used in computational mathematics, physics, computer vision, and other fields to solve problems involving dynamic boundaries, such as fluid dynamics, image processing, and material science. A level set function is a function that takes positive and negative signs, which can be used to represent a partition of the domain Ω into two disjoint regions Ω_1 and Ω_2. Let $\phi:\Omega\to R$ be a level set function, then its signs define two disjoint regions

$$\Omega_1=\{x:\phi(x)>0\}, \quad \Omega_2=\{x:\phi(x)<0\} \quad (8)$$

If the regions that must be partitioned are more than two regions, we must use two or more level set functions to represent the regions separately. In Li *et al.*,[25] the authors introduced three phase level set functions for image segmentation, and we briefly introduce their work because we use this in the segmentation of corona CT images. In fact, the CT images of the lung can be segmented into three parts: healthy parts, which are in black color in CT images; the corona, which involves areas that are like gray clouds; and the outer part of the lung, or other things with white color. Therefore, using the three-phase method can be useful. To better guide the movement of the gradient in the level set method, we have used the shearlet transform, which is a more accurate recent work.

In this case of a two-phase problem, a level set function ϕ is used to represent the two regions Ω_1 and Ω_2 given by (8). The regions Ω_1 and Ω_2 can be represented with their membership functions defined by $M_1(\phi)=H(\phi)$ and $M_2(\phi)=1-H(\phi)$ respectively, where is the Heaviside function. Thus, for the case of two-phase (N=2), the energy function can be as the following level set formulation:

$$\varepsilon=\int\sum_{i=1}^{N}\left(\int K(y-x)\left|I(x)-b(y)c_i\right|^2 dy\right)M_i(\phi(y))dx \quad (9)$$

Where $K(y-x)$ is introduced as a nonnegative window function, also called the kernel function. I is image, and b is the bias field, and each c_i denotes the boundary of each region. By minimizing this energy, we obtain the result of image segmentation represented by the level set function and the bias field estimation. Energy minimization is performed through an iterative process. In each iteration, we minimize the energy with respect to each variable b and c_i, given the other two updated in the previous iteration.

In the case of three-phase (N=3), we use two-level set functions ϕ_1 and ϕ_2 to get three membership functions as:

$$M_1(\phi_1,\phi_2)=H(\phi_1)H(\phi_2), M_2(\phi_1,\phi_2)=H(\phi_1)(1-H(\phi_2))$$

and $M_3(\phi_1,\phi_2)=1-H(\phi_1)$ to give a three-phase level set formulation. For more details about the three-phase level set method and its numerical application, see Li *et al.*[25]

Proposed Scheme

Since, in the multiphase level set, the boundaries of areas (c_1,c_2) move based on the gradient value of pixels, finding a consistent edge guiding method is necessary. Because shearlet transform keeps the edges coherent among the introduced edge detection method, we have used it in the following Algorithm. In fact, we give an edge guiding scheme based on shearlet transform coefficients of pixels and similarity measurement of those coefficients.

Algorithm 1

1. Take an image, namely (*I*)
2. Compute the shearlet transform of the image in each direction
3. For each point, assume a neighborhood 5 × 5. For the center point x_{00} and its neighborhoods, the similarity measurement C is obtained as follows:

$$C = \frac{g_{a,s}(\xi)}{g_{a,s}(x_{00})} \tag{10}$$

In formula (10), $g_{a,s}(x_{00})$ is the shearlet transform in direction *s* and scale *a* at the central point (x_{00}). $g_{a,s}(\xi)$ is the weighted mean value of the gradient of the neighborhood of x_{00}, it can be computed as follows:

$$g_{a,s}(\xi) = \frac{\sum_{i,j=1}^{i,j=5} \omega_{i,j} g_{a,s}(\xi)}{\sum_{i,j=1}^{i,j=5} \omega_{i,j}} \tag{11}$$

Where, $\omega_{i,j} = \frac{e^{-d_{ij}}}{d_{ij}}$. Each d_{ij} in (11) can be found in the following matrix for the neighborhood of each central point.

$$\begin{bmatrix} 0.0072 & 0.0165 & 0.0234 & 0.0165 & 0.0072 \\ 0.0165 & 0.0594 & 0.1270 & 0.0594 & 0.0165 \\ 0.0234 & 0.1270 & 0 & 0.1270 & 0.0234 \\ 0.0165 & 0.0594 & 0.1270 & 0.0594 & 0.0165 \\ 0.0072 & 0.0165 & 0.0234 & 0.0165 & 0.0072 \end{bmatrix}$$

(Note that each value in this matrix is associated with each neighborhood distance from the central point because closer points are more efficient.) By using this matrix, the effect of the distance of each pixel from the central pixel becomes more prominent in the edges of the gradient, and this matrix application can enhance the gradient of the image.

In case the denominator in formula (10) becomes zero, Eq. 10 can be modified as:

$$C = \frac{g_{a,s}(\xi)}{g_{a,s}(x_{00}) + 1} \tag{12}$$

By this work, there will be no dividing by zero in the MATLAB code. Moreover, for a better comparison, we set a constant *A* to widen the gaps between all values of C, as the following equation:

$$C = \frac{g_{a,s}(\xi) - A}{g_{a,s}(x_{00}) + 1} \tag{13}$$

4. After computing *C* values for all directions in each pixel, we sum all directions *C* and then divide the range of *C* into subranges. Therefore, the gradient of the image can be segmented into some subregions
5. For each subregion, we can automatically find threshold values, such as genetic algorithm,[26,27] and therefore, all edges in the image can be efficiently detected
6. After edge detection in each direction, we can sum all direction information for efficient segmentation and edge detection.

Next, because Algorithm 1 highlights prominent edges, in Algorithm 2, we use this algorithm to guide the gradient flow in the multiphase segmentation of CT images of lung-involved corona. We give a scheme for the affected lung area by coronavirus based on shearlet transform, contrast stretch transform, and three-phase level set. It is worth mentioning that if we need to highlight edges, we can use Algorithm 1, but when we want to show regions that are not very different from their neighborhoods, we use Algorithm 2 in the following, and use Algorithm 1 for guiding gradient flow in the multiphase segmentation method.

Algorithm 2

1. Take an image, namely (*I*)
2. Apply phase stretch transform on the image (*I*).[28] This work can significantly increase the difference between points with high frequencies and others
3. Compute the shearlet transform of the image obtained from step 2 to obtain the low-pass and high-pass images from Eq. 7
4. Apply contrast stretching on the low-pass image obtained from step 3. The contrast stretch transform of an image is the transform that expands the difference between the gray scales of the image in a suitable interval. Here, we have chosen the simple form of contrast stretching as follows:

$$P_{out} = (P_{in} - c)\left(\frac{b-a}{d-c}\right) + a \tag{14}$$

Where $[a,b] = [0,255]$ is the suitable interval and *c,d* are the minimum and maximum of the input image (P_{in}).

Compute the inverse shearlet transform of the image with a new low-pass image to obtain the contrast-stretched image. In the shearlet transform, the frequency space of the image (Fourier transform) is partitioned into several parts, as shown in Figure 1.

In Figure 1, the central part shows the low-pass filter, and the surrounding parts show the high-pass filter output. The difference between pixels has been increased by applying the contrast stretch transform on the low-pass part of the image. Then, by Inverse Fast Fourier Transform 2, we obtained a new original image to apply the multiphase level set on it and obtain better results.

5. Apply the multiphase level set to the contrast-stretched image obtained from step 4. By this, the lung CT image can be segmented into three parts: white, black, and gray. The gray part shows the involved area.

To clarify the interaction between Algorithm 1 and Algorithm 2, we explicitly replace the classical curvature term $(K_{curvature} = n_{xx} + n_{yy})$ in the level set evolution equation by the edge map (HT), which is derived from shearlet-based

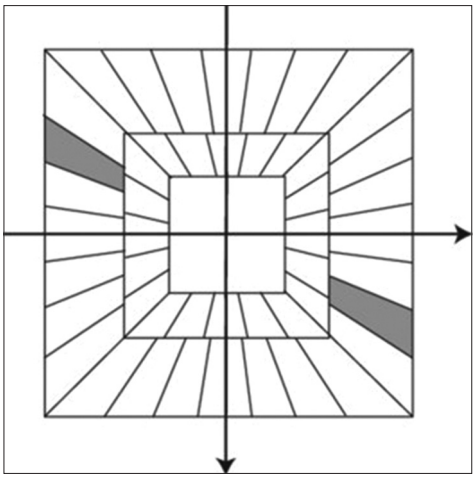

Figure 1: Division of the Fourier transform domain

edge detection in Algorithm 1. This substitution provides more robust edge guidance during multiphase segmentation, especially in low-contrast or noisy areas. The workflow diagram and a general pseudocode are shown in Figures 2 and 3, respectively.

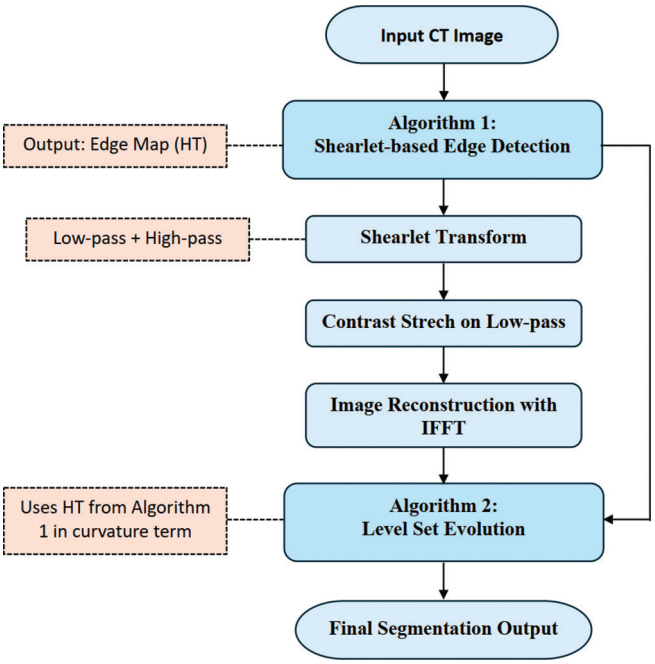

Figure 2: The workflow diagram

Results

In this section, we provided the visual result of the proposed algorithm on some medical images to indicate its good performance.

Figure 4 shows that Algorithm 1 effectively delineates edges. Furthermore, the curved regions exhibit closed forms, allowing for the use of active contours, where convergent contours can represent the affected areas.

Figure 5 demonstrates that Algorithm 1 better represents the tumor area than the Shearlet transform. Since our study focused solely on the tumor region and its boundaries, we restricted our comparison to the tumor area and its edges identified by Algorithm 1 and the tumor boundaries delineated by the Shearlet method. The differences between the two methods are evident in Figure 5, so we did not perform a quantitative comparison. The results of the proposed algorithm for edge detection are better than those of the shearlet approach.

Figure 6 shows the visual results of Algorithm 2. In fact, we have applied Algorithm 2 on each lobe, and then, by gathering each lobe's result beside each other, the segmentation result of the hole of the lung can be obtained. As can be seen, the contrast stretching transform can lead to better results than the shearlet approach. In the next figures [Figures 7 and 8], the result of each lobe is demonstrated separately.

Because by using level set or Algorithm 2 of this paper in experience in the whole of the image with one sigma, the corona affected area cannot be specified, and other regions' grayscale values can affect the average value in each iteration of the level set or Algorithm 2. Hence, we executed the second algorithm separately on each lung lobe to get exact results. The rationale behind this approach is the nonuniform intensity distribution across the lobes. Hence, by applying different sigma (the Gaussian distribution parameter) to each lobe, we achieved more accurate segmentation of the corona-affected regions compared to using a single sigma value for both lobes. This is clearly illustrated in Figures 7 and 8. The level set method in these figures cannot demonstrate the corona-affected areas exactly. Indeed, other areas unaffected by coronavirus are diagnosed as coronavirus areas. Moreover, some parts, such as corona-affected areas, cannot be detected, and so, it cannot detect corona-affected areas exactly. However, in these figures, Algorithm 2 can demonstrate that the corona areas are exactly separate from other areas of the lobes. For comparison between Algorithm 2 and the level set method, we have used the figure of merit (FOM) score. Indeed, the FoM score measures the accuracy of the detected edges within a region, with a range between 0 and 1. A higher value, closer to 1, indicates greater precision in the detected edges. The FoM score is computed using the following formula:

$$FoM = \frac{1}{\max\left(N_I, N_A\right)} \sum_{k=1}^{N_A} \frac{1}{1 + md^2\left(k\right)}$$

Where N_I denotes the number of actual edges, N_A represents the number of detected edges, m is the scaling constant set to $\frac{1}{9}$, and $d(k)$ is the distance between the actual edges and the corresponding detected edges.

Moreover, we have computed the dice similarity coefficient (DSC) for Algorithm 2 and the level set method. This parameter shows the overlap between the segmentation

Input: Original Image I

Step 1: Edge Guidance using Shearlets (Algorithm 1)
- Decompose image I using shearlet transform
- Apply adaptive thresholding to extract edge features
- Reconstruct edge map HT from significant shearlet coefficients

Step 2: Preprocessing for Level Set Segmentation
- Smooth the input image I (e.g., Gaussian filter)
- Initialize level set function u (e.g., random or based on mask)
- Initialize bias field b

Step 3: Level Set Evolution (Algorithm 2)
For each outer iteration:
For each inner iteration:
- Compute region-based terms C1, C2, C3
- Update bias field b
- Compute Heaviside and Dirac functions
- Compute energy gradient based on:
  Data fitting terms
  Regularization terms
  Edge guidance term using HT instead of curvature
- Update level set function u using:
  u = u + timestep * (FittingTerm + HT.* EdgeTerm)

Output: Segmented image with highlighted infected lung areas

Figure 3: Pseudocode: Integration of algorithm 1 and algorithm 2

results and the segmentation by experts. It can be computed from the following formulae:

$$DSC = \frac{2TP}{2TP + FP + FN}$$

Where, TP is true positive, FP is false positive, and FN is false-negative pixels in segmentation. Table 1 shows FOM and DSC values for Algorithm 2 and the level set method.

It shows that Algorithm 2 can detect regions closer than level set to exact regions and overlaps more exact corona regions. The proposed segmentation method processes each CT image in approximately 15 s, including edge enhancement and region detection stages. In comparison, state-of-the-art deep learning-based approaches often require significantly longer processing times. For example, in the study by Mali *et al*.,[29] the authors reported a processing time of nearly 1 h per CT image due to the large image size and deep neural network complexity. Similarly, in the study by Shan *et al*.,[30] the authors used a human-in-the-loop deep learning system and reported a processing time of approximately 4 min per CT volume. These comparisons indicate that the proposed method provides a competitive trade-off between speed and accuracy, especially for environments with limited computational resources.

Discussion and Conclusion

With COVID-19 still affecting many across the globe, lung involvement detection in COVID-19 is critical for

Figure 4: Visual results of the edge detection for the proposed scheme (Algorithm 1)

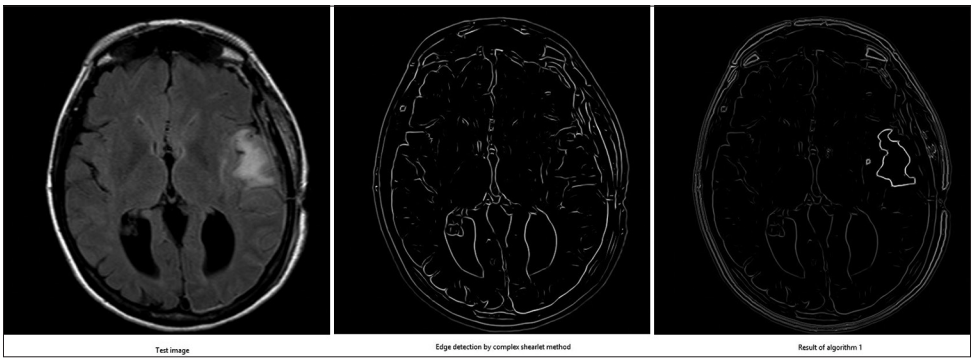

Figure 5: Visual results of the edge detection for the proposed scheme (Algorithm 1)

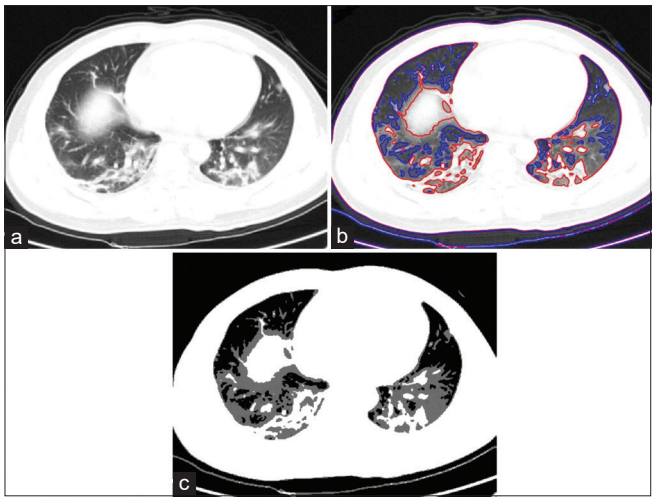

Figure 6: (a) original image, (b) the result of Algorithm 2, (c) segmented regions by different phases obtained from Algorithm 2

understanding disease severity and guiding treatment. In this paper, we have used a new scheme for edge guiding of the images in Algorithm 1, and then, we have used it in Algorithm 2 for the segmentation of corona-involved areas. The first scheme was based on the shearlet transform of pixels and their similarity measurement. Thanks to the shearlets' strength in keeping the coherence of the edges, using them was more efficient than other edge detectors. Collecting the information obtained from all directions, we can get outstanding results in segmentation because each direction contributes to a gradient associated with its influence. Figures 4 and 5 indicate that by using Algorithm 1, the boundaries of the images are prominent rather than other areas and are bolded from other weak boundaries. In the second algorithm, we have applied contrast stretch transform with shearlet transform for edge detection. Through these works, we have obtained good results for

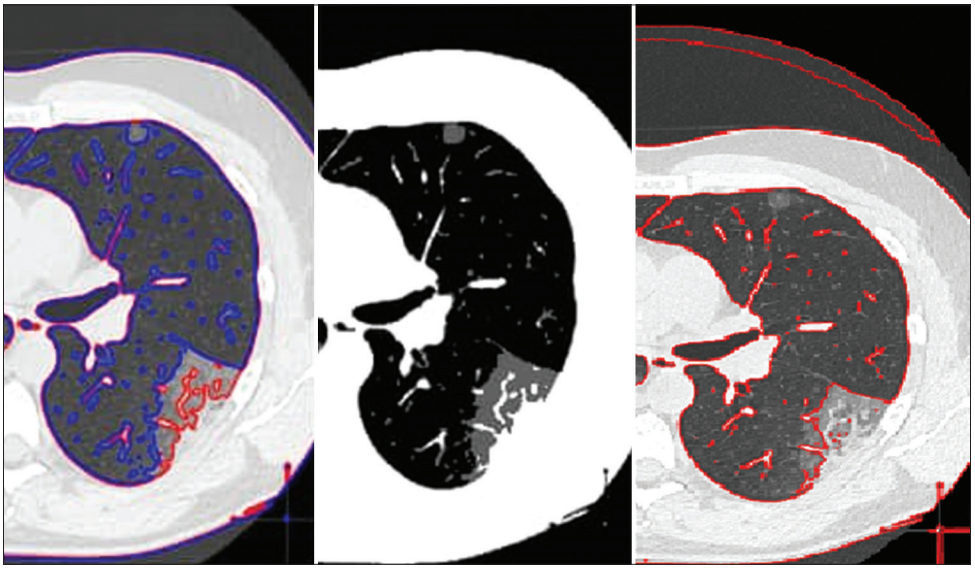

Figure 7: From left to right: Results of Algorithm 2 applied to the right lung lobe. The segmented image, where each color represents a phase (sigma = 50). Result of the level set method

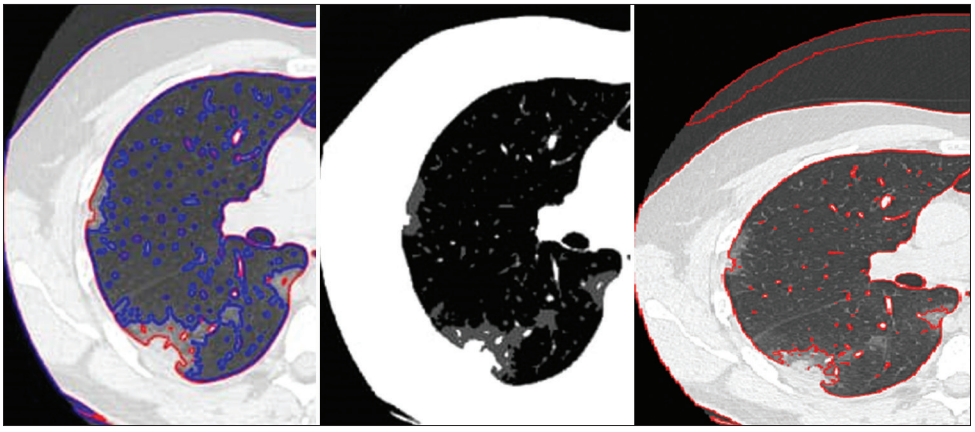

Figure 8: From left to right: Results of Algorithm 2 applied to the left lung lobe. The segmented image, where each color represents a phase (sigma = 40). Result of the level set method

Table 1: Figure of merit and dice similarity coefficient comparison between the level set and Algorithm 2

Method	Level set	Algorithm 2
FOM	0.34	0.91
DSC	0.19	0.94

FOM – Figure of merit; DSC – Dice similarity coefficient

edge detection using shearlets. The algorithm has been tested on 500 images. The proposed method demonstrates strong performance in segmenting COVID-19-infected regions with a high accuracy FoM = 0.91, DSC = 0.94. Furthermore, we have used the method in extracting involved areas of the lung with coronavirus in about 15 s for better and faster involved area detection. When working with neural networks in image processing, the large size of medical images often results in long processing times. For instance, in the paper "Automatic Detection of Lung Infected COVID-19 Disease Using Deep Learning" by Mali *et al.* (2021),[29] published in Nonlinear Analysis: Applications, Vol. 12, pp. 921–929, the reported processing time is approximately 1 h. In comparison, our method significantly reduces this time to just 15 s.

In Figure 6, the affected areas by coronavirus form separate phases, which can be seen in the gray color in segmented images. Stretching the phase leads to exact results. Using shearlets has multiplied this effect. We conclude that using the proposed multi-phase method, we can correctly obtain the lung areas affected by coronavirus pneumonia, and by using the shearlet transform, the boundary of GGO areas can be shown clearly. Figures 7 and 8 reveal that applying the second algorithm separately to each lung lobe and adjusting the sigma value for the Gaussian function results in more accurate segmentation of each lobe than using a single, fixed sigma value for the entire image. Moreover, the comparison between the original level set method and Algorithm 2 in terms of quantity and quality in Figures 7 and 8 and Table 1 shows that Algorithm 2 shows exact results rather than the level set method. In fact, using a multiphase algorithm, a separate phase can demonstrate the corona areas, and using a shearlet modified by Algorithm 1, the guiding edge of the regions can be done more carefully. In future work, we plan to focus on reducing processing time and expanding this algorithm to handle 3D images.

Ethical approval

This study was conducted in accordance with institutional and national ethical guidelines. The CT scan data were provided by Ayatollah Taleghani Hospital in Urmia with all patient identifiers removed prior to analysis.

Funding

No funding was received to assist with the preparation of this manuscript.

Availability of data and materials

The CT images used in this study were obtained from Ayatollah Taleghani Hospital in Urmia and are not publicly available due to patient privacy and institutional restrictions. However, derived data, processed results, and implementation code supporting the findings of this study are available from the corresponding author upon reasonable request.

Financial support and sponsorship

Nil.

Conflicts of interest

There are no conflicts of interest.

References

1. Benmalek E, Elmhamdi J, Jilbab A. Comparing CT scan and chest X-ray imaging for COVID-19 diagnosis. Biomed Eng Adv 2021;1:100003.
2. Aslan MF. A robust semantic lung segmentation study for CNN-based COVID-19 diagnosis. Chemometr Intell Lab Syst 2022;231:104695.
3. Chakraborty S, Mali K. SUFEMO: A superpixel based fuzzy image segmentation method for COVID-19 radiological image elucidation. Appl Soft Comput 2022;129:109625.
4. Hao S, Huang C, Heidari AA, Xu Z, Chen H, Alabdulkreem E, *et al*. Multi-threshold image segmentation using an enhanced fruit fly optimization for COVID-19 X-ray images. Biomed Signal Process Control 2023;86:105147.
5. Karar ME, Khan ZF, Alshahrani H, Reyad O. Smart iomt-based segmentation of coronavirus infections using lung CT scans. Alex Eng J 2023;69:571-83.
6. Madhavi M, Supraja P. COVID-19 infection prediction from CT scan images of lungs using iterative convolution neural network model. Adv Eng Softw 2022;173:103214.
7. Kalaivani S, Seetharaman K. A three-stage ensemble boosted convolutional neural network for classification and analysis of COVID-19 chest x-ray images. Int J Cogn Comput Eng 2022;3:35-45.
8. Bishop CM, Nasrabadi NM. Pattern Recognition and Machine Learning. Vol. 4. New York: Springer, 2006.
9. Li Z, Zhao G, Li S, Sun H, Tao R, Huang X, *et al*. Rotation feature extraction for moving targets based on temporal differencing and image edge detection. IEEE Geosci Remote Sensing Lett 2016;13:1512-6.
10. Hong S, Kim J, Rivera AR, Song G, Chae O. Edge Shape Pattern for Background Modeling Based on Hybrid Local Codes. In: 2016 13th IEEE International Conference on Advanced Video and Signal Based Surveillance (AVSS). IEEE; 2016. p. 1-7.
11. Noras P, Aghazadeh N. Directional schemes for edge detection based on b-spline wavelets. Circuits Syst Sign Process 2018;37:3973-94.
12. Gu J, Pan Y, Wang H. Research on the improvement of image edge detection algorithm based on artificial neural network. Optik 2015;126:2974-8.
13. Arandjelović O, Cipolla R. A methodology for rapid illumination-invariant face recognition using image processing filters. Comput Vision Image Underst 2009;113:159-71.
14. Gimenez J, Martinez J, Flesia AG. Unsupervised edge map

scoring: A statistical complexity approach. Comput Vision Image Underst 2014;122:131-42.
15. Marr D, Hildreth E. Theory of edge detection. Proc R Soc Lond B Biol Sci 1980;207:187-217.
16. Kong H, Sarma SE, Tang F. Generalizing laplacian of gaussian filters for vanishing-point detection. IEEE Trans Intell Transp Syst 2013;14:408-18.
17. Canny J. A computational approach to edge detection. IEEE Trans Pattern Anal Mach Intell 1986;8:679-98.
18. Goswami JC, Chan AK. Fundamentals of Wavelets, Theory, Algorithms, and Applications. Wiley Series in Microwave and Optical Engineering. John Wiley & Sons; 2011.
19. Mallat S, Zhong S. Characterization of signals from multiscale edges. IEEE Trans Pattern Anal Mach Intell 1992;14:710-32.
20. Guo K, Kutyniok G, Labate D. Sparse multidimensional representations using anisotropic dilation and shear operators. Wavelets Splines 2006;14:189-201.
21. Yi S, Labate D, Easley GR, Krim H. A shearlet approach to edge analysis and detection. IEEE Trans Image Process 2009;18:929-41.
22. Aghazadeh N, Moradi P, Noras P. Constructing multiwavelet-based shearlets and using them for automatic segmentation of noisy brain images affected by COVID-19. J Med Signals Sens 2023;13:183-90.
23. Mirzafam M, Aghazadeh N. A three-stage shearlet-based algorithm for vessel segmentation in medical imaging. Pattern Anal Applic 2021;24:591-610.
24. Osher S, Sethian JA. Fronts propagating with curvature-dependent speed: Algorithms based on Hamilton-Jacobi formulations. J Comput Phys 1988;79:12-49.
25. Li C, Huang R, Ding Z, Gatenby JC, Metaxas DN, Gore JC. A level set method for image segmentation in the presence of intensity inhomogeneities with application to MRI. IEEE Trans Image Process 2011;20:2007-16.
26. Goldberg DE. Genetic algorithms in search, optimization, and machine learning, Addison-Wesley, USA; 1989.
27. Griffiths A JF., Doebley J, Peichel C, Wassarman D. Introduction to Genetic Analysis 12ed, W. H. Freeman; 2020.
28. Asghari MH, Jalali B. Edge detection in digital images using dispersive phase stretch transform. Int J Biomed Imaging 2015;2015:687819.
29. Mali H, Alameady H, Fahad A, Abdullah A. Automatic detection lung infected COVID-19 disease using deep learning (convolutional neural network). Int J Nonlinear Anal Appl 2021;12:921-9.
30. Shan F, Gao Y, Wang J, Shi W, Shi N, Han M, *et al*. Lung infection quantification of COVID-19 in CT images with deep learning. arXiv:2003.04655, 2020.